

## Supporting Information

*for*

### **Comprehensive Insights into the Multi-Antioxidative Mechanisms of Melanin Nanoparticles and Their Application To Protect Brain from Injury in Ischemic Stroke**

Yanlan Liu,<sup>†, ‡, †</sup> Kelong Ai,<sup>†, †</sup> Xiaoyuan Ji,<sup>‡</sup> Diana Askhatova,<sup>‡</sup> Rose Du,<sup>§</sup> Lehui Lu,<sup>\*, †</sup> and Jinjun Shi<sup>\*, ‡</sup>

<sup>†</sup>State Key Laboratory of Electroanalytical Chemistry, Changchun Institute of Applied Chemistry, Chinese Academy of Sciences, Changchun 130022, China

<sup>‡</sup>Center for Nanomedicine and Department of Anesthesiology, Brigham and Women's Hospital, Harvard Medical School, Boston, MA 02115, USA

<sup>§</sup>Department of Neurosurgery, Brigham and Women's Hospital, Harvard Medical School, Boston, MA 02115, USA

\*To whom correspondence should be addressed. E-mail: lehuilu@ciac.ac.cn (L.L.) or jshi@bwh.harvard.edu (J.S.)

<sup>†</sup>These authors contributed equally to this work.

## **Materials and Methods**

### **Materials**

Dopamine hydrochloride, ammonium hydroxide solution, ethanol, 5-diethoxyphosphoryl-5-methyl-1-pyrroline N-oxide (DEPMPO), peroxidase from horseradish (HRP), superoxide dismutase bovine (SOD), crown ether, Rhodamine B, antimycin A,  $\text{CoCl}_2$ ,  $\text{KO}_2$ ,  $\text{H}_2\text{O}_2$ , Poly(ethylene glycol) bis(3-aminopropyl) terminated were purchased from Sigma-Aldrich. NOC7 was purchased from Dojindo Molecular Technologies, Inc. Amine-terminated polyethylene glycol with PEG molecular weight 5000 (mPEG5k-NH<sub>2</sub>) was obtained from Nanocs Inc. Alexa Fluor 488 phalloidin was purchased from Life Technologies. Antibodies used in this work were from Cell Signaling or Abcam.

### **Synthesis and characterization of PEG-functionalized melanin nanoparticles (PEG-MeNPs)**

MeNPs were prepared according to a method previously reported.<sup>1</sup> Briefly, a mixture containing ammonia aqueous solution (2.5 mL,  $\text{NH}_4\text{OH}$ , 28-30%), ethanol (40 mL) and deionized water (90 mL) was stirred at 30 °C for 30 min. Dopamine hydrochloride aqueous solution was then slowly injected into the above mixture, and the reaction was allowed to proceed under mild stirring for 24 h. Thereafter, MeNPs were isolated by centrifugation and washed with water three times.

Amine-terminated polyethylene glycol (mPEG5k-NH<sub>2</sub>) was conjugated onto the surface of MeNPs through Schiff base and/or Michael addition reactions. Briefly, 50 mg of MeNPs were dispersed in the Tris buffer (10 mM, pH 8.5), and 125 mg of mPEG5k-NH<sub>2</sub> was added. The reaction was allowed to proceed for 12 h under vigorous stirring at room temperature. The PEG-MeNPs were isolated by centrifugation, washed with deionized water for three times to remove the residual PEG, and then re-dispersed in deionized water for further investigations.

The morphology of PEG-MeNPs was characterized with Tecnai G2 Spirit BioTWIN transmission electron microscope (FEI Company) operating at 80 kV. XRD spectra were recorded with a D8 ADVANCE (Germany) using Cu-Ka (0.15406 nm) radiation. XPS measurements were conducted with a VG ESCALAB MKII spectrometer. The size of PEG-MeNPs in the serum-containing medium was determined by Dynamic Light Scattering or DLS (15-mW laser, incident beam of 676 nm; Brookhaven Instruments Corporation). FTIR measurements were performed with a MET-10-PerkinElmer FT-IR system. The  $^1\text{H}$  NMR spectra were recorded with a Mercury VX-300 spectrometer at 400 MHz (Varian, USA), using  $\text{D}_2\text{O}$  as a solvent and TMS as an internal standard. The UV-Vis spectra were recorded with a VARIAN CARY 50UV-Vis spectrophotometer.

### **Spin-trap free radical scavenging**

5-diethoxyphosphoryl-5-methyl-1-pyrroline N-oxide (DEPMPO) was used as the trapper for  $\text{O}_2^{\bullet-}$  and  $\bullet\text{OH}$  radicals. The stock solution of  $\text{O}_2^{\bullet-}$  radicals was produced by dissolving  $\text{KO}_2$  in DMSO/crown ether (0.2 M), which was stored at  $-80\text{ }^\circ\text{C}$  and used within several weeks. For electron paramagnetic resonance (EPR) measurements, the  $\text{KO}_2$  solution was added into a PBS solution containing EDTA (0.2 mM), DEPMPO (40 mM), and PEG/MeNPs/PEG-MeNPs/SOD/water, and the EPR spectra were recorded.  $\bullet\text{OH}$  radicals were generated by the Fenton reaction using  $\text{H}_2\text{O}_2$  and  $\text{CuCl}$ .

### **Catalysis of $\text{O}_2^{\bullet-}$ dismutation by PEG-MeNPs**

The production of molecular oxygen in the  $\text{KO}_2$  solution with and without PEG-MeNPs was measured using an YSI 5000 dissolved oxygen meter. The formation of  $\text{H}_2\text{O}_2$  was measured by the Amplex Red assay. Briefly, 38  $\mu\text{L}$  of  $\text{NaOH}$  (5 mM) was added into the  $\text{KO}_2$  working solution (2 mL) in the absence or presence of PEG-MeNPs, and allowed to react for 5 or 30 min.

The mixture was then added to TAPS buffer (100 mM, pH 8.2) containing Amplex Red (40  $\mu$ M) and HRP (10 U/mL). The absorbance of the resofurin produced was measured using a UV-Vis spectrophotometer. The pH value changes were monitored by using a pH meter after addition of  $\text{KO}_2$  or KOH to the aqueous solution in the absence or presence of PEG-MeNPs.

### **$\bullet$ NO and ONOO<sup>-</sup> scavenging by PEG-MeNPs**

The  $\bullet$ NO scavenging ability of PEG-MeNPs was tested by EPR using carboxy-PTIO (Sigma-Aldrich) as the trapper and detection dye for  $\bullet$ NO. NOC7 was used as the source of  $\bullet$ NO. For the EPR test, carboxy-PTIO was dissolved in phosphate buffer (250 mM, pH 7.4), and NOC7 was dissolved in NaOH (1 mM). In a test tube, 0.5% methylcellulose was mixed with NOC7 (5  $\mu$ M) for 30 min at room temperature, and the mixture was then added into the carboxy-PTIO solution (5  $\mu$ M) in the absence or presence of PEG-MeNPs. The EPR spectra were then recorded. The EPR signal of carboxy-PTIO is characterized by five lines.  $\bullet$ NO generated from NOC7 can reduce carboxy-PTIO into carboxy-PTI, which shows seven-line EPR signals. In addition, the reduction of carboxy-PTIO by  $\bullet$ NO will lead to a color change from purple to yellow.

The ONOO<sup>-</sup> scavenging ability of PEG-MeNPs was evaluated by UV-Vis spectroscopy using pyrogallol red as the indicator.

### **Cell culture**

Neuro 2A cells and Raw 264.7 macrophage cells were purchased from ATCC and cultured in Dulbecco's Modified Eagle Medium (DMEM) (ATCC) supplemented with 10% (v/v) FBS with high glucose, and maintained at 37  $^{\circ}$ C in 5%  $\text{CO}_2$  and a humidified atmosphere.

### ***In vitro* cytotoxicity of PEG-MeNPs**

Alamar Blue assay and LDH assay (Life Technologies) were performed to evaluate cell viability. Briefly, Neuro 2A cells were seeded in 96-well plates at a density of 20,000 cells/well for 24 h. The cells were then treated with PEG-MeNPs at different concentrations for another 24 h. Cells were counted by Alamar Blue assay according to the manufacturer's instructions. For LDH assay, optical absorbance at 490 nm and 680 nm was measured using a microtiter plate reader. Maximum LDH Activity Control was obtained by cell lysis with DMSO. Relative LDH release was calculated according to the methods provided by the manufacturers.

For analysis of mitochondrial function, Neuro 2A cells were seeded in 96-well plates at a density of 20,000 cells/well for 24 h, and treated with different concentrations of PEG-MeNPs. Twenty-four hours later, the ATP levels in different groups were measured using a mitochondrial toxicity assay (Promega) according to the manufacturer's instructions.

### **Intracellular RONS scavenging by PEG-MeNPs**

For the ROS scavenging study *in vitro*, Neuro 2A cells were seeded in 96-well plates, and pretreated with PEG-MeNPs at different concentrations overnight before adding antimycin A (10  $\mu\text{g}/\text{mL}$ ) or  $\text{CoCl}_2$  (0.3 mM).  $\text{O}_2^{\bullet-}$  and ROS in the cells were measured using MitoSOX (Life Technologies) and 2',7'-dichlorodihydrofluorescein diacetate ( $\text{H}_2\text{DCFDA}$ , Life Technologies), respectively, according to the manufacturer's instructions.

To evaluate the anti-inflammatory activities of PEG-MeNPs, Raw 264.7 cells were seeded in 96-well plates for 24 h, and incubated with PEG-MeNPs at different concentrations, followed by LPS treatment. Intracellular ROS and RNS levels were measured using  $\text{H}_2\text{DCFDA}$  and Griess reagent (Sigma), respectively. Cells were also collected for western blot analysis.

### **Western blot analysis**

Protein extracts were prepared using modified radioimmunoprecipitation assay lysis buffer (50 mM Tris-HCl pH 7.4, 150 mM NaCl, 1% NP-40 substitute, 0.25% sodium deoxycholate, 1 mM sodium fluoride, 1 mM Na<sub>3</sub>VO<sub>4</sub>, and 1 mM EDTA), supplemented with protease inhibitor cocktail (Cell Signaling) and 1 mM phenylmethanesulfonyl fluoride. The concentration of protein in the extracts was measured with a bicinchoninic acid (BCA) protein assay kit (Pierce/Thermo Scientific) according to the manufacturer's instructions. 30 µg protein was loaded on SDS-PAGE gels and transferred to nitrocellulose or polyvinylidenedifluoride membranes. Thereafter, the membranes were blocked with 3% BSA in TBST (50 mM Tris-HCl, pH 7.4, 150 mM NaCl, and 0.1% Tween 20) and then incubated with appropriate primary antibodies at 4 °C overnight. After washing, the membranes were incubated with HRP-conjugated secondary antibodies at room temperature for 1 h. Signals were measured using the enhanced chemiluminescence (ECL) detection system (Pierce).

### **Immunofluorescence staining**

For immunofluorescence experiments, after treatment with PEG-MeNPs and stimulation with LPS or CoCl<sub>2</sub>, cells were washed with PBS twice and fixed with 4% paraformaldehyde at room temperature for 10 min. After washing with PBS for three times (5 min each), the cells were permeabilized by incubation in 0.2% Triton X-100 in PBS for 5 minutes on ice, followed by washing with PBS twice (5 min each). The cells were then blocked with blocking buffer (2% normal goat serum, 2% BSA and 0.2% gelatin in PBS) at room temperature for 1 h, washed with PBS for three times (5 min each), and incubated with the appropriate diluted primary antibody for 1 h at room temperature. After washing with PBS, the cells were incubated with diluted fluorescent dye-linked secondary antibody with/without dye-labeled phalloidin (Life Technologies) for 1 h, washed with PBS, stained with Hoechst 33342 for 1 min, and finally

mounted on slides with Prolong Gold antifade mounting medium (Life Technologies). Fluorescence images were obtained using a Leica DM-IRE2 inverted fluorescence microscope (Leica Microsystems).

## **Animals**

Animal handling procedures were in accordance with National Institutes of Health animal care guidelines for all *in vivo* experiments. All animal housing, care, and experiments were performed according to the guidelines and regulations of the Institutional Animal Care and Use Committee.

## **Rat models of the ischemic stroke**

Male Wistar rats (250-300 g) were randomly divided into three groups: saline control, NP-treated group, and sham group (15 rats per group), anesthetized by intraperitoneal administration of ketamine (80 mg/kg) and xylazine (40 mg/kg) and then placed in a stereotaxic frame. 8  $\mu$ l of saline or PEG-MeNP solution (10 mg/mL) in saline was then injected into the right lateral ventricles (AP: -0.8mm, ML: -1.4 mm, DV: -3.6 mm) of rats at a rate of 0.5  $\mu$ l/min. After injection, the needle was left for an additional 5 min before withdrawal. Focal cerebral ischemia was induced according to the method previously reported, with a minor modification.<sup>2</sup> Briefly, under anesthesia, the skin on the neck was sterilized and a midline incision was made. The common carotid artery was isolated from the surrounding tissues and exposed at its bifurcation. The external carotid artery and common carotid artery were ligated using a silk suture. Thereafter, a 5-0 nylon monofilament suture was rounded by heating and inserted into the common carotid artery. After 90 min of occlusion, the rats were sacrificed and the brains were collected for further analysis. Only scalp incisions were made in the sham group under anesthesia.

### **TTC staining of brain tissues**

The brain of each rat was harvested, washed with saline, and then sectioned coronally into five slices (2-mm-thick, from rostral to caudal). Thereafter, the brain slices were added into a PBS solution (pH 7.4) containing 2% of 2,3,5-triphenyltetrazolium chloride (TTC) (Sigma-Aldrich), and incubated at 37 °C for 20 min. After TTC staining, the slices were fixed in 4% paraformaldehyde solution (Sigma-Aldrich) for imaging and quantification analysis.

### **Detection of $O_2^{\bullet-}$ *in vivo***

The brain of each rat was harvested, weighted, and frozen quickly in PBS (pH 7.4) using liquid nitrogen for future use. To examine the level of  $O_2^{\bullet-}$ , the brain tissues were homogenized in PBS (pH 7.4) after thawing, and the supernatant was collected from the brain homogenate through centrifugation at a speed of 2000-3000 rpm/min for 20 min. The level of  $O_2^{\bullet-}$  in brains was then detected by using the superoxide anion assay kit (Nanjing Jiancheng Bioengineering Institute) according to the manufacture's instruction.

### **Hematologic examination and histology**

For the *in vivo* toxicity study, healthy C57BL/6 mice were intravenously administered PEG-MeNP solution (10 mg/mL). Blood was collected by a retro-orbital puncture and serum was separated for blood biocompatibility test. Organs including brain, heart, liver, spleen, lung, and kidney were harvested, fixed in a 10% formalin solution, and embedded in paraffin for hematoxylin and eosin (H&E) staining.

To assess the blood biocompatibility of PEG-MeNPs, red blood cells were isolated by centrifugation at 2000 g/min for 10 min and washed with PBS five times, and then diluted 10-fold with PBS. 0.1 mL of red blood cell solution was then added into 0.4 mL of PBS (negative



control), deionized water (positive control), or PBS solutions containing different concentrations of PEG-MeNPs, and incubated at room temperature for 3 h. After centrifugation at 14800 rpm/min for 20 min, the absorbance of the supernatants at a wavelength of 541 nm was determined using a microplate reader. Hemolysis of PEG-MeNPs was calculated according to the following equation:

$$\text{Hemolysis\%} = (A_{\text{sample}} - A_{(-)\text{control}}) / (A_{(+)\text{control}} - A_{(-)\text{control}})$$

Where  $A$  is the absorbance of the sample at a wavelength of 541 nm.

### **Immune response**

C57BL/6 mice were intravenously injected with 200  $\mu$ l of saline or PEG-MeNP solution (10 mg/mL) through the tail vein. At 4 h and 24 h post-injection, blood was collected and serum was isolated through centrifugations at 2000 g/min for 10 min. The levels of cytokines in the serum samples including IFN- $\gamma$ , TNF- $\alpha$ , IL-12, and IL6 were measured by enzyme-linked immunosorbent assay (ELISA) (Life Technologies) according to the manufacturer's instructions.

### **Statistical analysis**

All data are presented as their means with S.D., unless otherwise noted. Statistical significance was determined by a two-tailed Student's  $t$  test assuming equal variance. A  $p$  value  $<0.05$  is considered statistically significant. Statistical values are indicated in figures according to the following scale: \* =  $p < 0.05$  and \*\* =  $p < 0.01$ .

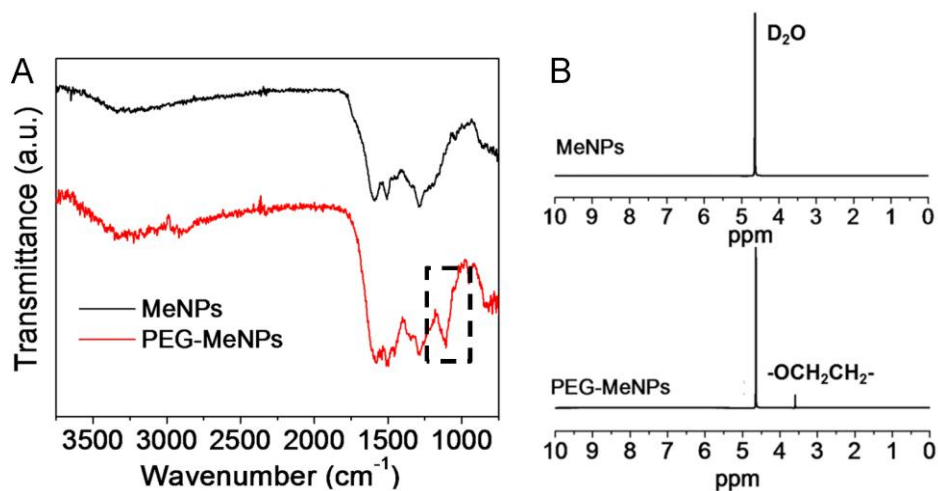


**Figure S1.** FTIR spectra (A) and <sup>1</sup>H NMR spectra (B) of MeNPs and PEG-MeNPs, respectively. The peak at ~1110 cm<sup>-1</sup> in the FTIR spectrum is attributed to the C-O-C stretching of PEG on the surface of PEG-MeNPs. The new peak at ~3.6 ppm in the <sup>1</sup>H NMR spectrum is attributed to the -OCH<sub>2</sub>CH<sub>2</sub>- of PEG on the surface of PEG-MeNPs.

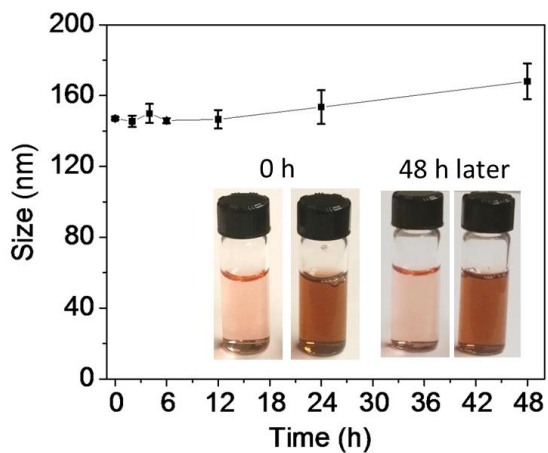


**Figure S2.** Size change of PEG-MeNPs in the serum-containing cell culture medium over 48 h. The insert is the picture of free medium and PEG-MeNP-containing medium at 0 vs. 48 h.

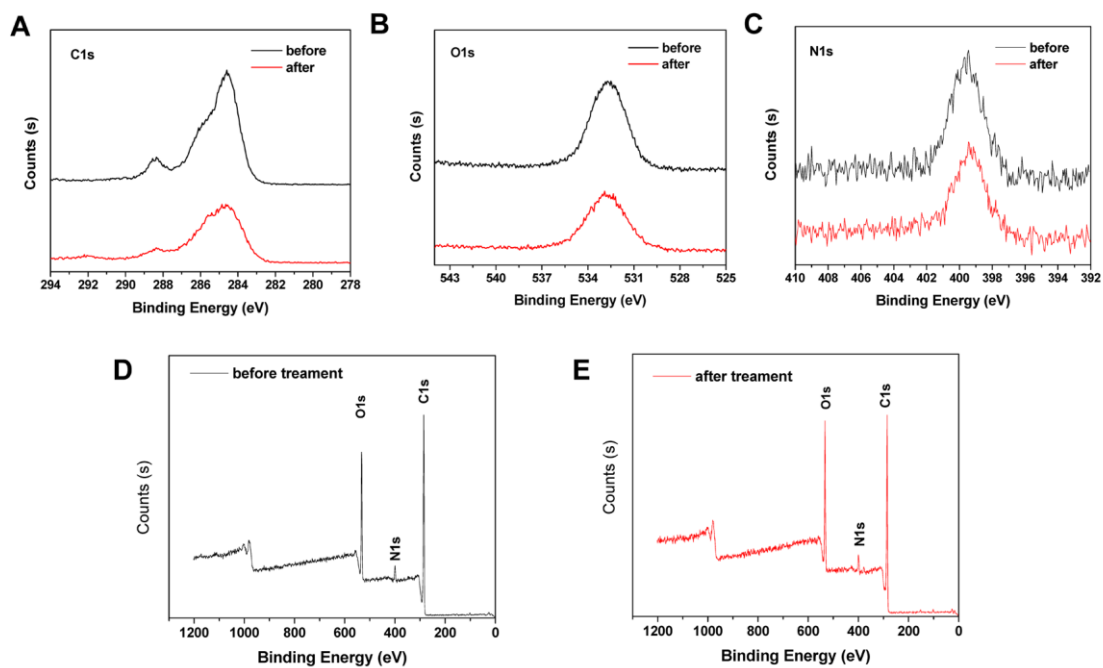


**Figure S3.** (A) C1s, (B) O1s, and (C) N1s analysis of PEG-MeNPs before and after treatment with  $\text{KO}_2$ . (D) and (E) are the survey spectra of PEG-MeNPs before and after treatment with  $\text{KO}_2$ , respectively.

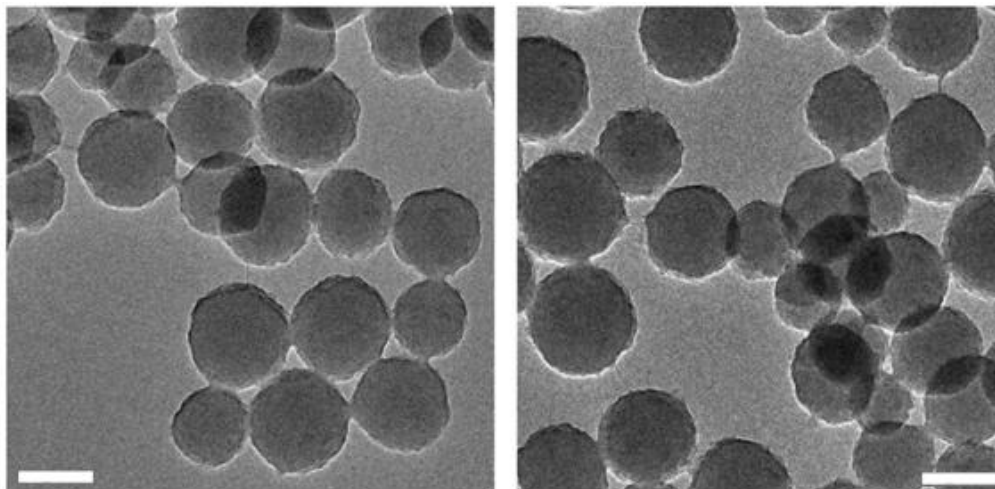


**Figure S4.** TEM images of PEG-MeNPs before (left) and after (right) treatment with  $\text{KO}_2$ . The scale bar is 100 nm.

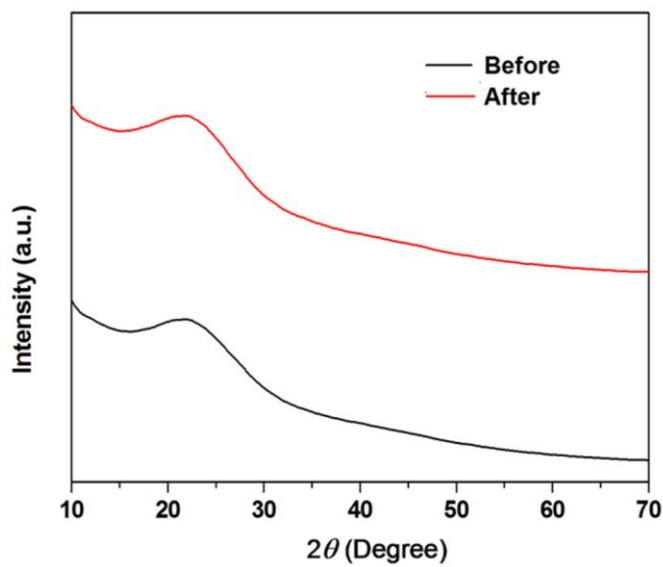


**Figure S5.** XRD spectra of PEG-MeNPs before and after treatment with  $\text{KO}_2$ .

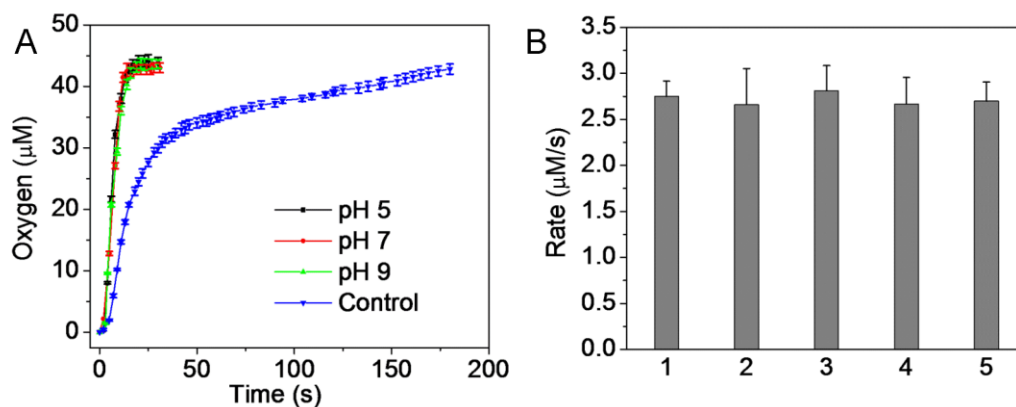


**Figure S6.** (A)  $O_2$  production from the  $KO_2$  solution in the absence or presence of PEG-MeNPs at different pH values. (B) Reaction rates of  $O_2^{\bullet-}$  dismutation catalyzed by different batches of PEG-MeNPs under the same conditions. The concentrations of PEG-MeNPs and  $KO_2$  are 0.1 nM and 100  $\mu$ M, respectively.

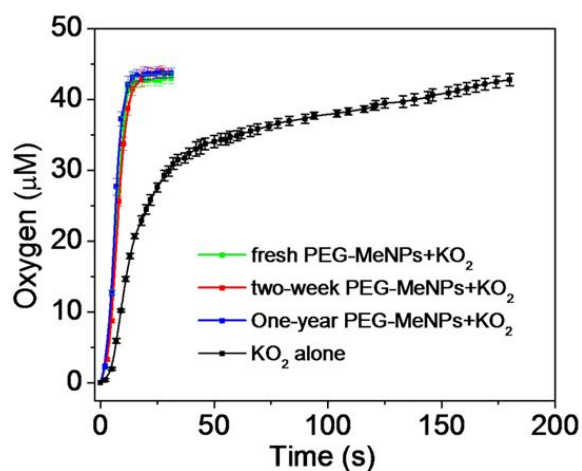


**Figure S7.**  $O_2$  production from the  $KO_2$  solution without PEG-MeNPs vs. with freshly prepared PEG-MeNPs, and PEG-MeNPs after storage at 4  $^{\circ}$ C for two weeks or one year. The concentrations of PEG-MeNPs and  $KO_2$  are 0.1 nM and 100  $\mu$ M, respectively.

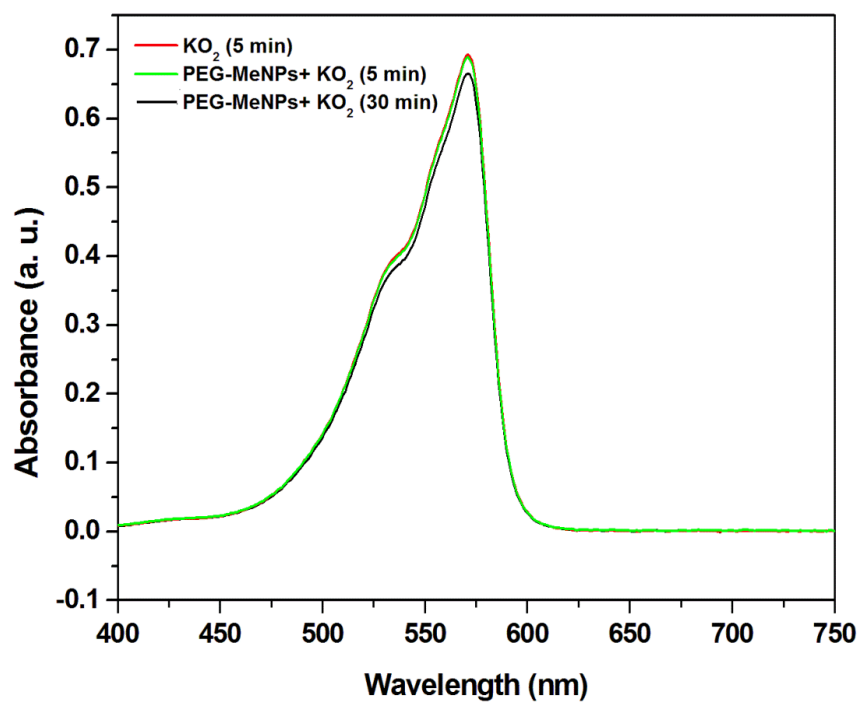


**Figure S8.** The absorbance change of the mixture of Amplex Red and HRP induced by KO<sub>2</sub> in the absence vs. presence of PEG-MeNPs (0.1 nM).

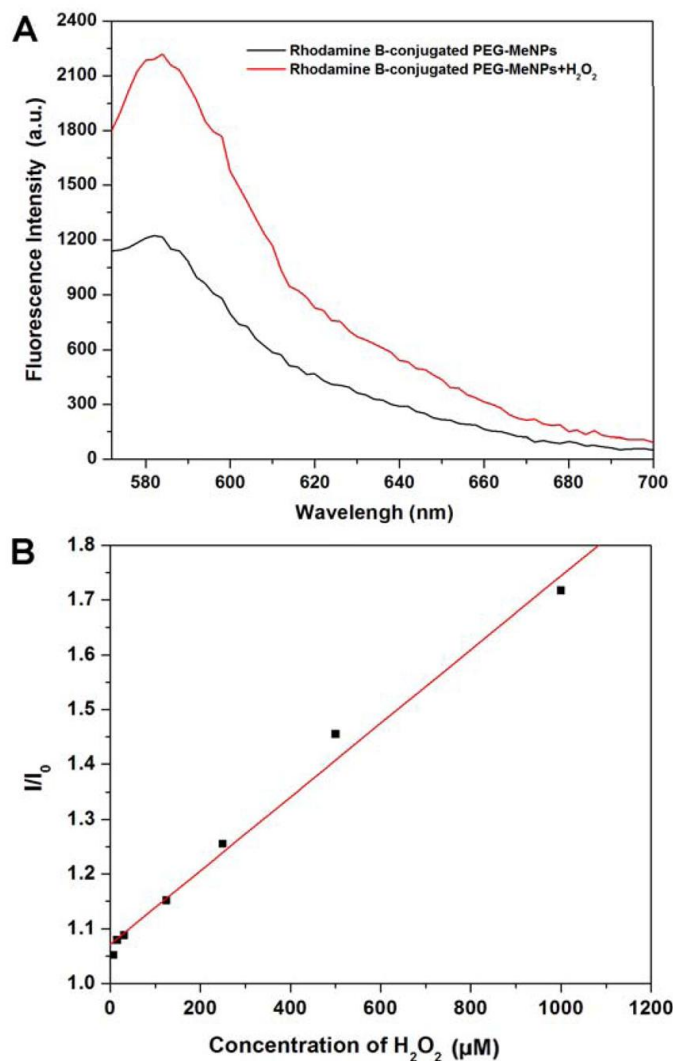


**Figure S9.** (A) Representative fluorescence spectra of Rhodamine B-conjugated PEG-MeNPs before vs. after reaction with H<sub>2</sub>O<sub>2</sub>. (B) Fluorescence intensity changes of Rhodamine B-conjugated PEG-MeNPs upon reaction with different concentrations of H<sub>2</sub>O<sub>2</sub>.  $I_0$  represents the original fluorescence intensity of the Rhodamine B-conjugated PEG-MeNP solution before reaction with H<sub>2</sub>O<sub>2</sub>, and  $I$  represents the fluorescence intensity of the Rhodamine B-conjugated PEG-MeNP solution after reaction with H<sub>2</sub>O<sub>2</sub>. We postulated that the decreasing of H<sub>2</sub>O<sub>2</sub> as indicated in Figure S8 was the result of the reaction between PEG-MeNPs and H<sub>2</sub>O<sub>2</sub>, as melanin in human hairs is known to be bleached by H<sub>2</sub>O<sub>2</sub>. To confirm this, Rhodamine B was covalently conjugated to the surface of PEG-MeNPs. Without H<sub>2</sub>O<sub>2</sub>, the fluorescence of Rhodamine B was significantly quenched *via* the Förster resonance energy transfer (FRET) effect between MeNPs and the fluorophore, whereas dose-dependent recovery of fluorescence was observed after adding H<sub>2</sub>O<sub>2</sub>. Given that the linkages among MeNPs, PEG, and Rhodamine were inert to H<sub>2</sub>O<sub>2</sub>, the fluorescence recovery can be explained by H<sub>2</sub>O<sub>2</sub>-induced etching of MeNPs and subsequent Rhodamine-PEG dissociation from the NP surface.

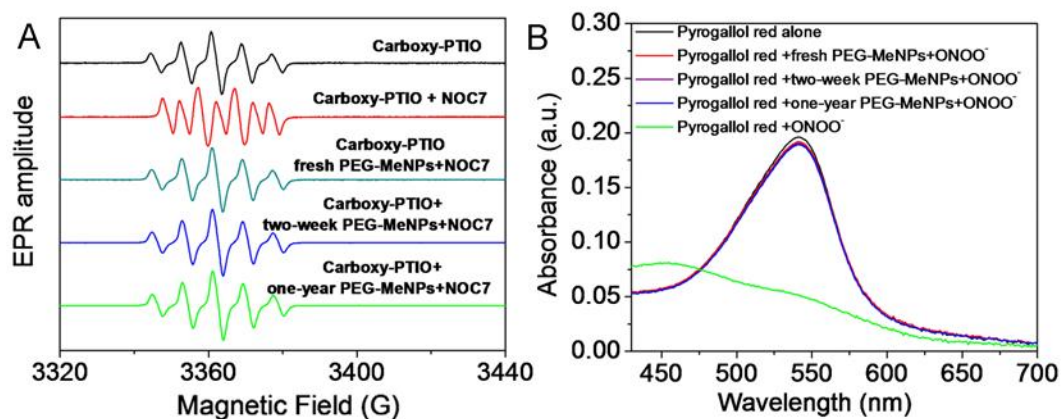


**Figure S10.**  $\bullet\text{NO}$  (A) and  $\text{ONOO}^-$  (B) scavenging effects of freshly prepared PEG-MeNPs (4 nM), and PEG-MeNPs (4 nM) after storage at 4 °C for two weeks or one year.



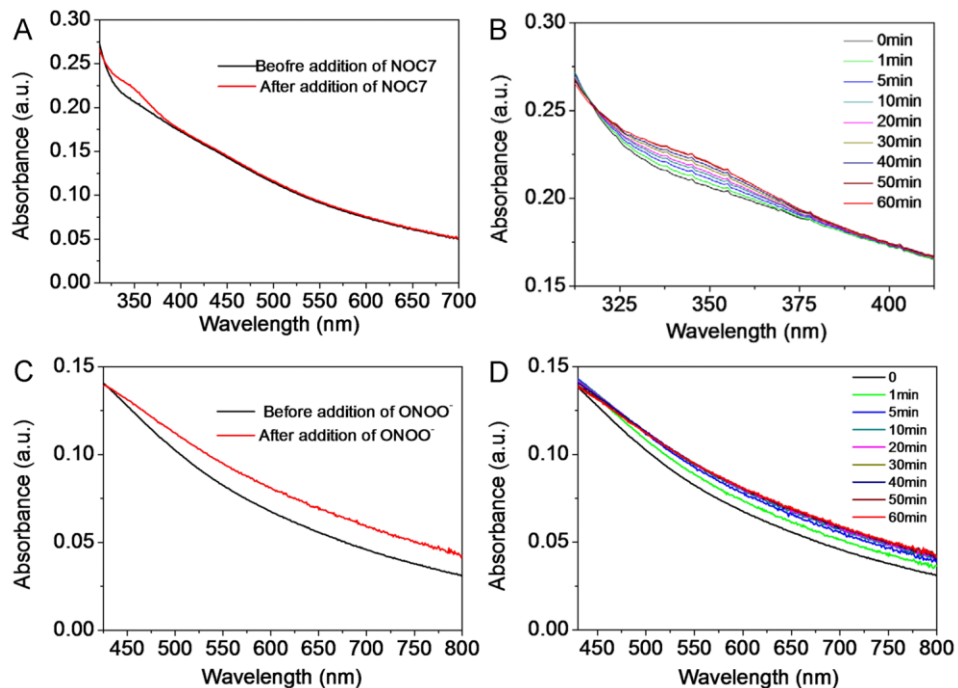


**Figure S11.** (A) UV-Vis spectra of the PEG-MeNPs solution after reaction with NOC7 for 1 h. (B) Time-dependent UV-Vis absorbance changes of the PEG-MeNPs solution after addition of NOC7. (C) UV-Vis spectra of the PEG-MeNPs solution after reaction with ONOO<sup>-</sup> for 1 h. (D) Time-dependent UV-Vis absorbance changes of the PEG-MeNPs solution after addition of ONOO<sup>-</sup>.

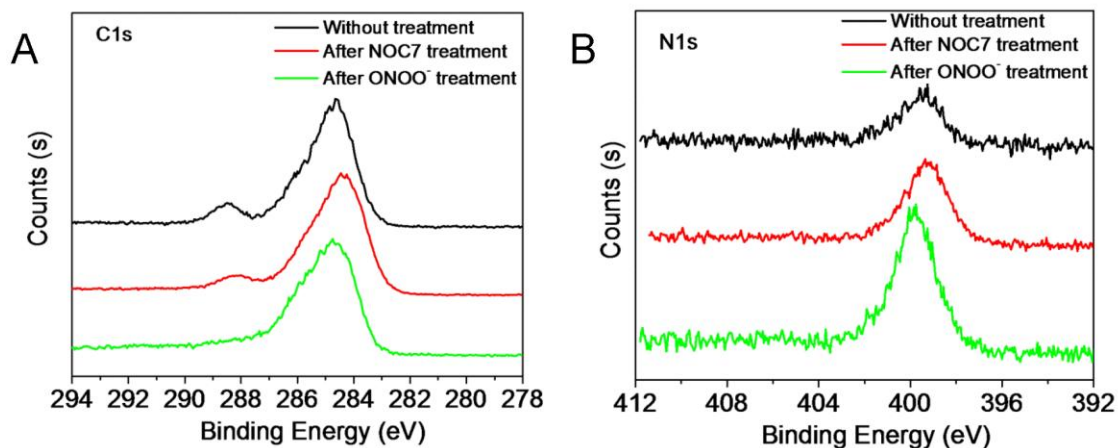


**Figure S12.** (A) C1s and (B) N1s analysis of non-treated PEG-MeNPs or PEG-MeNPs after treatment with NOC7 or ONOO<sup>-</sup>. After treatment with NOC7 or ONOO<sup>-</sup>, PEG-MeNPs showed an increased level of nitrogen, with no obvious change of carbon compared to the non-treated PEG-MeNPs.

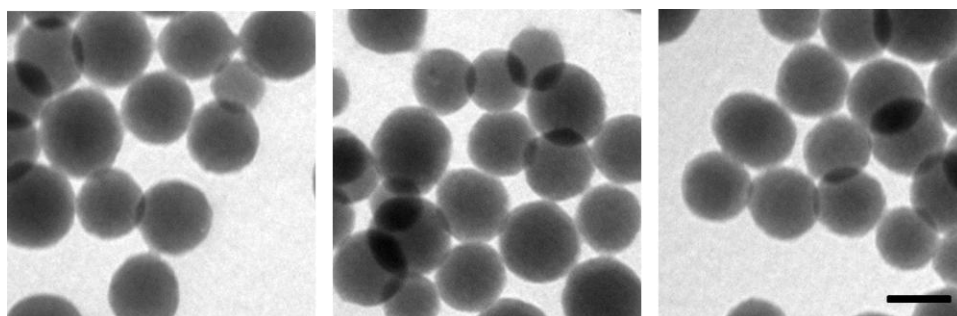


**Figure S13.** TEM images of non-treated PEG-MeNPs (left), PEG-MeNPs after treatment with NOC7 (middle) or ONOO<sup>-</sup> (right) for 1 h. The scale bar is 100 nm.

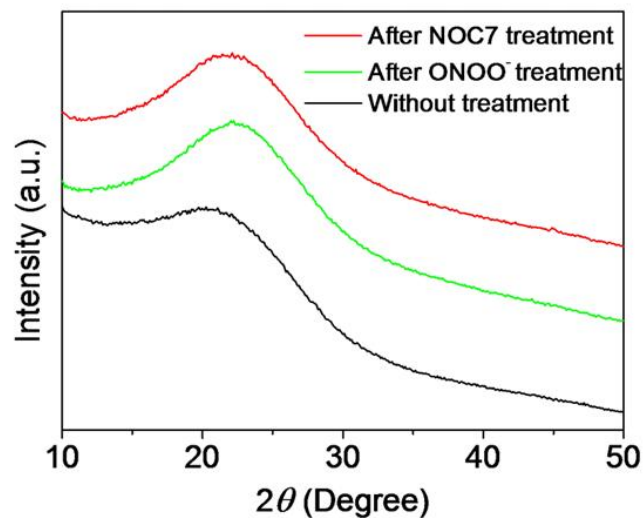


**Figure S14.** XRD spectra of non-treated PEG-MeNPs, and PEG-MeNPs after treatment with NOC7 or ONOO<sup>-</sup> for 1 h.

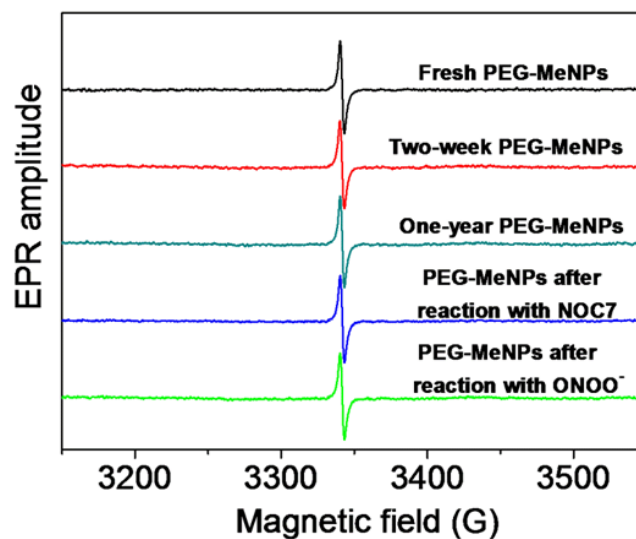


**Figure S15.** EPR spectra of fresh PEG-MeNPs, PEG-MeNPs after storage at 4 °C for two weeks or one year, or fresh PEG-MeNPs after reaction with NOC7 or ONOO<sup>-</sup>.

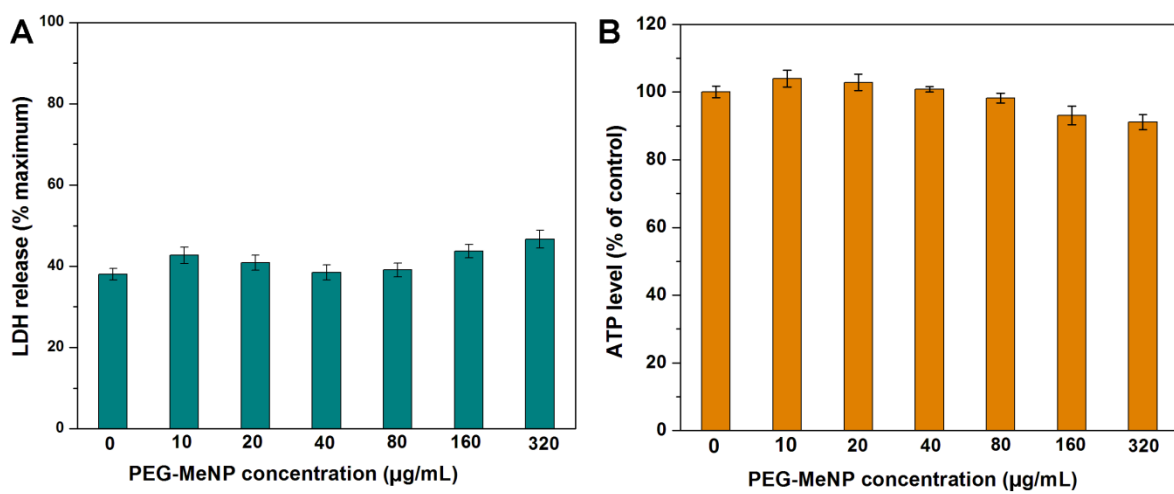


**Figure S16.** (A) LDH release and (B) ATP levels in Neuro 2A cells in the absence or presence of different concentrations of PEG-MeNPs.

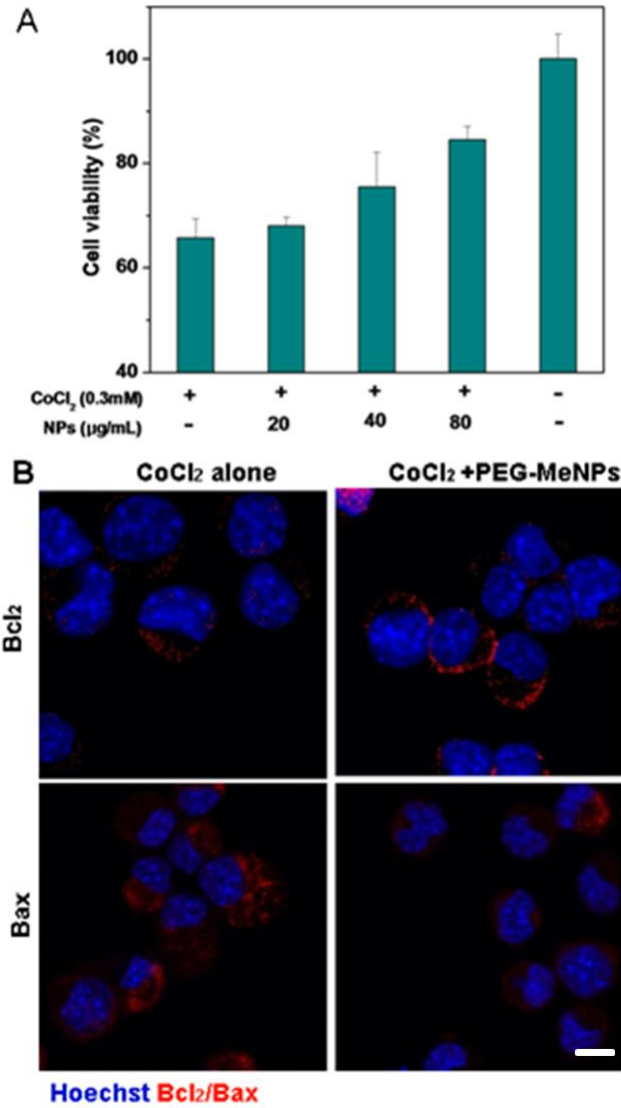


**Figure S17.** (A) Cell viability of and (B) immunofluorescence analysis of the expression of Bcl-2 and Bax in PEG-MeNP-pretreated Neuro 2A cells under the CoCl<sub>2</sub>-induced hypoxic condition (Scale bar, 10 µm).

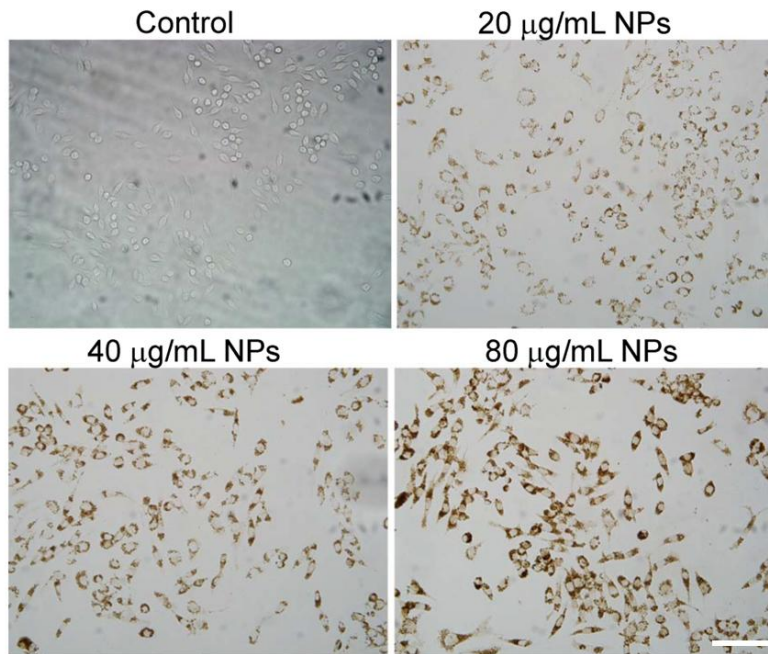


**Figure S18.** Uptake of PEG-MeNPs in Raw 264.7 macrophages (Scale bar, 100 μm).

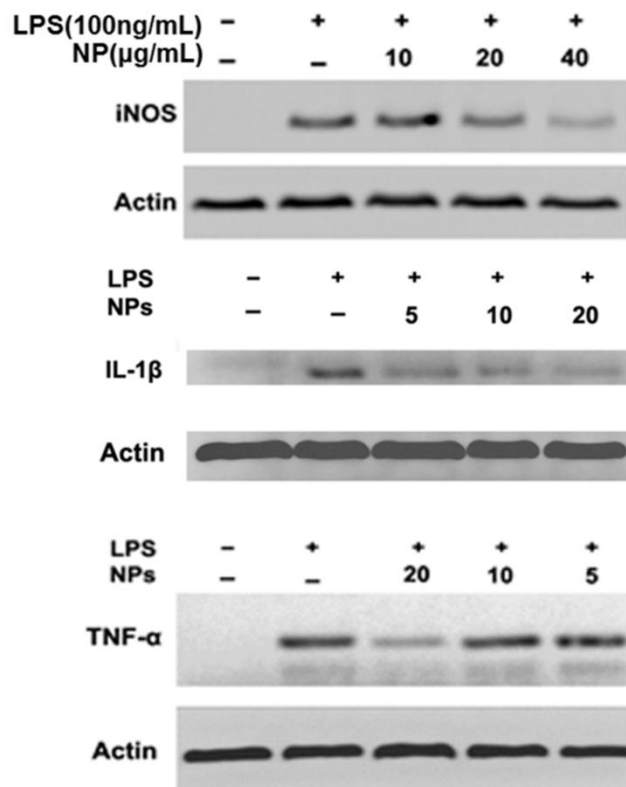


**Figure S19.** Western blot analysis of the expression of inflammatory mediators in LPS-treated macrophages in the absence or presence of PEG-MeNPs.

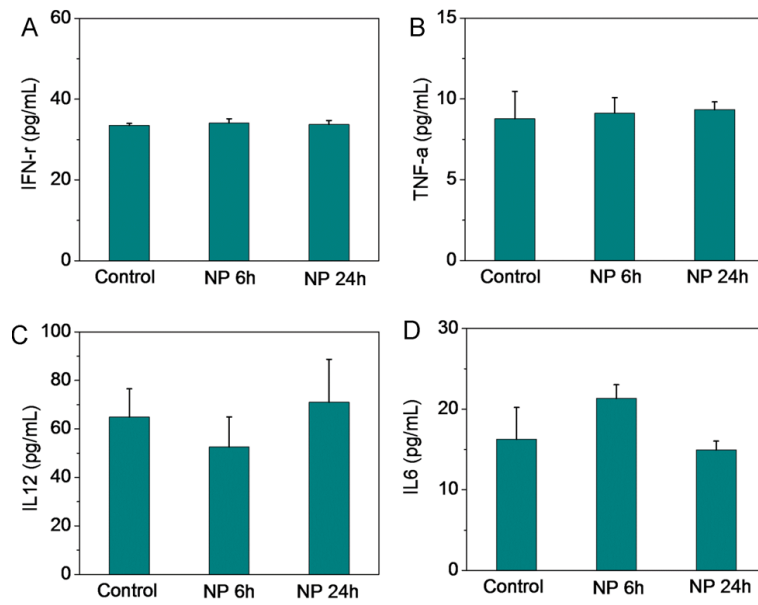


**Figure S20.** Cytokine response in mice at 6 h and 24 h post IV injection of PEG-MeNPs or PBS. Serum levels of (A) IFN- $\gamma$ , (B) TNF- $\alpha$ , (C) IL12, and (D) IL6.



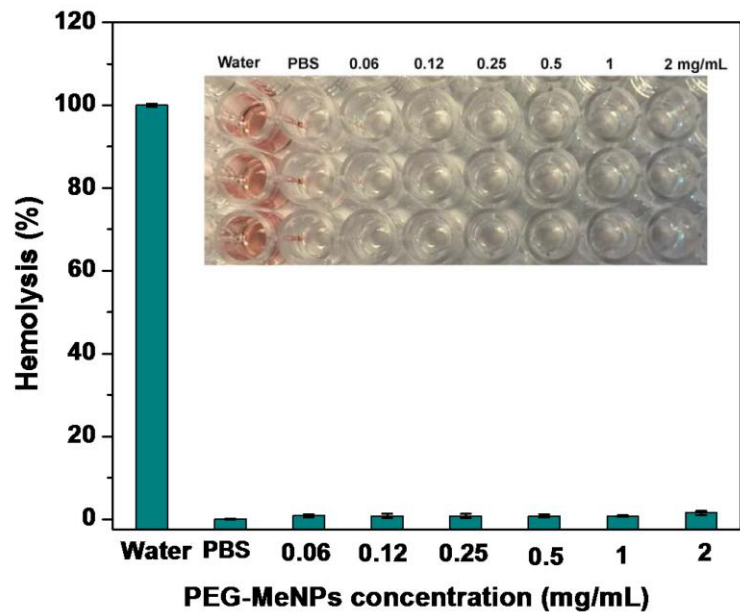


**Figure S21.** Hemolysis analysis of blood incubated with water (positive control), PBS (negative control), and different concentrations of PEG-MeNPs.

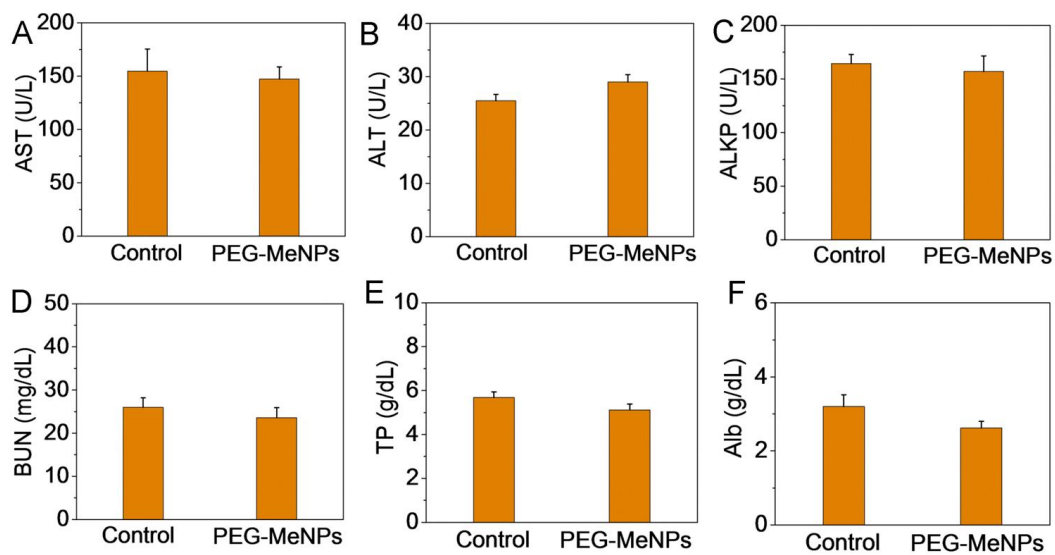


**Figure S22.** Serum levels of (A) aspartate aminotransferase (AST), (B) alanine aminotransferase (ALT), (C) alkaline phosphatase (ALKP), (D) blood urine nitrogen (BUN), (E) total protein (TP), and (F) albumin (Alb) in mice that received IV injection of PEG-MeNPs or saline control.

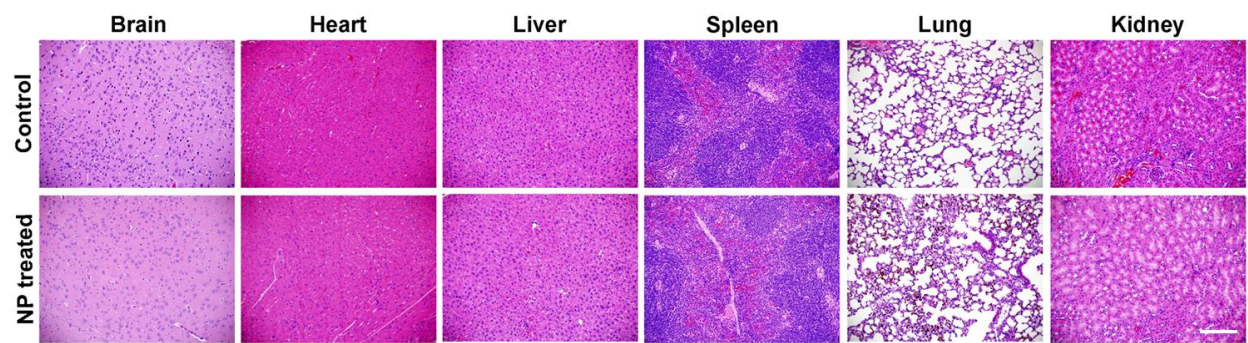


**Figure S23.** H&E staining of tissue sections of different organs including brain, heart, liver, spleen, lung, and kidney after treatment with PEG-MeNPs vs. saline control. Images were taken under 20 $\times$  objective (Scale bar, 100  $\mu$ m).

## References

- (1) Liu, Y.; Ai, K.; Liu, J.; Deng, M.; He, Y.; Lu, L. *Adv. Mater.* **2013**, *25*, 1353.
- (2) a) Kim, C. K.; Kim, T.; Choi, I. Y.; Soh, M.; Kim, D.; Kim, Y. J.; Jang, H.; Yang, H. S.; Kim, J. Y.; Park, H. K.; Park, S. P.; Park, S.; Yu, T.; Yoon, B. W.; Lee, S. H.; Hyeon, T. *Angew. Chem. Int. Ed.* **2012**, *51*, 11039; b) Lee, H. J.; Park, J.; Yoon, O. J.; Kim, H. W.; Lee, D. Y.; Kim do, H.; Lee, W. B.; Lee, N. E.; Bonventre, J. V.; Kim, S. S. *Nat. Nanotechnol.* **2011**, *6*, 121.